Online Multi-time Scale Energy Management Framework for Smart PV Systems with Mix of Fast and Slow System Dynamics

Daichi Watari[a,*], Ittetsu Taniguchi[a], Hans Goverde[b,c,d], Patrizio Manganiello[b,c,d], Elham Shirazi[b,c,d], Francky Catthoor[b,c], Takao Onoye[a]

[a]*Osaka University, 1-5 Yamadaoka, Suita, Osaka 565-0871, Japan*
[b]*imec, Kapeldreef 75, 3001 Heverlee, Belgium*
[c]*ESAT, KULeuven, Kasteelpark Arenberg 10, 3001 Heverlee, Belgium*
[d]*EnergyVille, Dennenstraat 7, B-3600 Genk, Belgium*

Abstract

In this paper, an online multi-time scale energy management framework for a smart Photovoltaic (PV) system is proposed, which can calculate optimized schedules of battery operation, power purchase, and appliance usage. The smart PV system is a local energy community that includes several buildings and households equipped with PV panels and batteries. The objective is to realize real-time scheduling and very accurate energy management for reducing the electric bill and keeping the energy balance in the smart PV system. The proposed framework employs a model predictive control (MPC) approach and multi-time scale structure composed of two-time scales: longer coarse-grained scale and shorter fine-grained scale. In contrast to the many already proposed energy management approaches, this alternative structure enables the management of the necessary mix of fast and slow system dynamics with reasonable computational time while maintaining high accuracy. Simulation results show that the proposed framework can reduce electric bill up to a maximum of 48.1% compared with baseline methods. Besides, the effectiveness of multi-time scale and the need for accurate system modeling in terms of PV forecasting and batteries are also demonstrated.

Keywords: Online Energy Management,, Multi-time Scale, Battery, Shiftable Appliance, PV Forecasting

1. Introduction

The reduction of CO2 emission and the realization of a sustainable future motivate a broader integration of renewable energy into the energy system. In particular, the use of renewable generators close to the demand-side instead of centralized generation can reduce transmission losses [1]. However, renewable energy sources such as solar and wind are usually small-scale and uncontrollable; thus, the temporal and spatial mismatch between renewable generation and electricity demand is becoming a practical issue. For tackling this issue, it is necessary to renovate the conventional power grid towards a smart energy system. The smart energy system is an advanced power system capable of making the system more resilient, energy-efficient, and eco-friendly by integrating renewable generation and demand control [2, 3].

To put the smart energy system into practice, an energy management system (EMS) has the most critical role [4]. The EMS has three main functions: (1) real-time monitoring of users energy usage by a smart meter, (2) scheduling and optimization of the operation of system components, and (3) optimizing an objective function which can be composed of one or more critical system criteria, such as the electric bill minimization, peak-cut, grid failure rate, ramp rate, and a total lifetime. The general goal of the EMS is to manage the energy balance between appliances, batteries, and supply power provided by the grid and by renewable sources such as solar energy [5, 6]. However, it has become clear that harnessing the unpredictability and short term variability of renewable sources is a difficult task. The EMS currently relies on the energy stored in batteries to deal with the fluctuations of the renewable sources [7, 8]. Hence, an improved battery modeling and proper incorporation of the workload-dependent storage aspects in the EMS are desirable. This also includes the local battery management system (BMS), which is typically present in battery pack systems [9]. On the other hand, the battery system is not the only aspect that should be addressed.

The time scale of the control sequence of the EMS is a non-negligible factor in the performance of EMS. In practice, most smart system contexts exhibit a mix of fast and slow dynamics, which puts too high stress on the run-times when accuracy should also be maintained. For a long time scale up to a few days, the EMS application should consider a daily change of renewable generation and electricity demand. Furthermore, demand control (e.g., appliance scheduling) is usually performed daily or hourly frequency. It effectively matches the demand-supply in the local energy community, including several buildings and homes with many appliances. On the contrary, for a short time scale with a time resolution of a few seconds, the real-time energy imbalance between renewable generation and demand can directly cause energy loss. Therefore, it is neces-

*Corresponding author. E-mail address: watari.daichi@ist.osaka-u.ac.jp (D. Watari), Tel: +81-6-6879-4528, Fax: +81-6-6879-4529.

sary to precisely control the battery's operation based on forecast information on the expected renewable generation for compensating for real-time change of energy balance. As described above, the time scale that should be managed by the EMS to properly control the system varies widely, and the purpose of the different time scales also differs. Thus, when accuracy should not be sacrificed, and an EMS design suitable for each purpose and each time scale is required to meet all these criteria simultaneously. This problem is tackled in this paper employing a multi-time scale energy management framework.

Many researchers have focused on optimizing energy management for homes, buildings, or communities to schedule the battery system and electricity demand. The comprehensive home energy management system (HEMS) that includes thermal and energy storage to minimize cost and maximize comfort was studied in [10]. Celik et al. [11] worked on sharing photovoltaic (PV) generation in neighborhood homes, scheduling the use of appliances and batteries in the day-ahead. The energy co-scheduling framework in an office building to schedule a hybrid energy storage system (HESS) and heating, ventilating, and air conditioning (HVAC) was developed in [12]. As in [13], a ventilating system was optimized to control indoor air quality and energy consumption by a model predictive control (MPC) approach with an estimation of model parameters. In [14], the distributed algorithm by exchanging information with its neighbors to find the optimal dispatch of energy storage for a smart grid was proposed. The mixed-integer non-linear programming based EMS, which considers long-term energy efficiency programs and day-ahead energy storage scheduling, was formulated in [15]. In [16], a hybrid robust-stochastic optimization in HEMS was proposed to take the uncertainty of both day-ahead and real-time energy markets into consideration. Rocha et al. [17] employed artificial intelligence approaches such as the support vector machine and genetic algorithm to predict renewable generation and optimize the battery and demand operation. A multi-agent-based heuristic optimization to meet different consumer's energy demand in the renewable energy distribution network was proposed in [18]. In [19], a voting-based EMS and a rule-based controller in solar-wind-biomass hybrid energy systems were developed, improving demand-supply balance. Besides, the appliance commitment problems determine the best schedule to shift or shave the demand peak and fit for the electricity pricing policy [20, 21]. Lu et al. [22] proposed a mixed-integer linear programming (MIP) method to realize appliance scheduling with precise time-step and investigated the impact of PV energy storage systems. Although much literature has studied the scheduling of battery systems and demand, they are almost concerned with coarse-grain single-scale. They do not consider short-term PV fluctuations or battery's transient response, which are fast dynamics. Furthermore, the characteristics or problems of the battery have not been fully considered, which includes the I-V relationship, transient response, and state-of-charge (SOC) simulation.

In addition to the above literature, several studies have proposed the EMS considering multi-time scales. Abreu et al. [23] proposed a hierarchical MPC method to manage a set of different sub-systems such as appliances and load. Its upper layer calculates the maximum power limit, and its lower layer individually optimizes load schedules; however, the paper considers no renewable energies and no batteries. As in [24], the author also proposed a hierarchical control method focusing on a building, a battery system, and PV generation. A scheduling layer with 7 hours horizon and a pilot layer with 5 minutes horizon were integrated. In [25], a hierarchical EMS in an office building, containing PV systems and batteries of electric vehicles, was developed while dealing with day-ahead schedules and intra-hour adjustment. However, in these papers, the appliance scheduling is not fully considered, and the demand flexibility is limited. Also, the PV forecasting model is relatively simple, and short-term PV fluctuation is not entirely considered. In [26], a hierarchical two-layer HEMS to reduce daily electric bill and increase PV self-consumption was proposed. In the upper layer, the scheduling of the battery system and the appliances is performed for the next 24 hours. Although the lower layer is a rule-based real-time controller that compensates for PV fluctuation, it is relatively simple algorithm based on no short-term PV forecast data. The importance of accurate PV forecasting in energy management has been proved in the literature, and it has a significant effect on EMS performance [27, 28]. Finally, all of these papers do not have a detailed view of the PV forecasting and the battery state in seconds - minutes levels. The combination of them in the inner time loop is crucial for the accurate management of the supply-demand balance.

In this paper, an online multi-time scale energy management framework is developed for a smart PV system exhibiting such a mix of fast and slow dynamics. The smart PV system is the local community with several buildings and homes equipped with batteries, PV panels, and controllable appliances. For implementing online and real-time control, the MPC approach is employed together with accurately forecasting of PV generation and the latest battery state. We also introduce a detailed battery model that captures I-V characteristics and state-of-charge (SOC) accurately to realize precise energy management in the smart PV system. Besides, the multi-time scale structure of the proposed framework successfully treats fast and slow system dynamics on energy management in one integrated optimization loop by dividing the time scale into two-time scales, which are coarse-grained and fine-grained time scale. In this way, the modeling capability and computational time are improved. The effectiveness of the proposed framework is also validated via simulations. The results show that the proposed framework allows for saving in the electric bill up to 48.1% compared to baseline methods. Also, it is shown that the computational time is short enough to allow real-time control of smart PV systems. Furthermore, the effect of PV forecasting error and battery capacity is explored.

This paper is structured as follows: Firstly, the overview of the proposed framework and multi-time scale structure are given in Section 2. Section 3 shows the introduced systems models in detail. After that, the mathematical formulation of an online multi-time scale optimization problem is described in Section 4. Finally, the effectiveness of the proposed method is demonstrated via simulations with measured data in Section 5, and then Section 6 shows a summary of this paper.

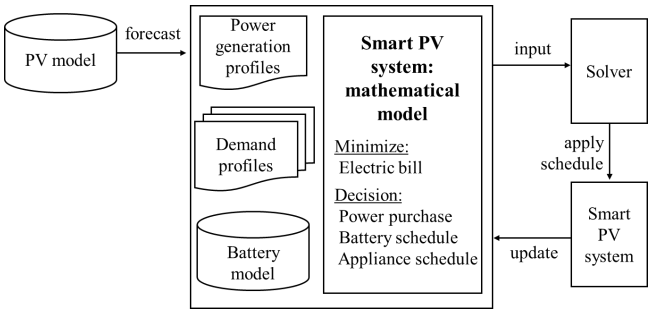

Figure 1: Online multi-time scale optimization framework for smart PV systems

2. Online Multi-time Scale Energy Management Framework

This section shows the overview of the proposed framework employing a model predictive control approach, namely an online multi-time scale energy management framework. The key ideas of the multi-time scale structure are also discussed in this section.

2.1. Overview of proposed framework

Figure 1 shows an overview of the proposed framework. The overall objective is to minimize the electric bill. The input of this framework is electric demand information and forecasting data of PV generation. The output of the framework is an operation plan that includes power purchase from the utility grid, battery charge/discharge, and appliance schedules. To realize online energy management, we utilize the MPC approach in the proposed framework. The MPC is an effective means of dealing with control problems that have many variables [29], and recent works have successfully applied MPC to the energy management problem [24, 30]. The key idea of MPC is the iteration of forecasting and optimization. The future control inputs over the planning period are obtained by solving an optimization problem based on forecast information and predicted system behavior. The only first-sample solution is applied, after that, the planning period recedes, and the above processes are iterated. It should be stressed that the MPC approach can potentially compensate for the uncertainty of a variation of load demand and generation because of its feedback structure [31]; therefore, we apply the MPC to the energy management framework.

The main processes of the proposed framework based on the MPC approach are iterated as follows. First, the framework obtains the PV power forecasting data in the near future, such as the upcoming half an hour a few days. Then the framework optimizes the energy utilization in order to minimize the electric bill from the utility grid. The energy utilization includes battery charge/discharge, power purchase, and appliance schedule. This optimization problem is mathematically formulated, and a mathematical solver can obtain the optimal results. Finally, the obtained plan is applied to the system operation. In this way, the latest information on systems is reflected, and online control interpolating energy balance is realized.

2.2. Multi-time scale structure

The main idea of a multi-time scale structure is to solve one integrated optimization loop that covers the two-time scales, called coarse-grained time scale and fine-grained time scale. These time scales take into account appliance scheduling, a variation of demand load and PV generation, and accurate battery characteristics. Firstly, the coarse-grained time scale is responsible for energy management in a long-term period (up to a few days) with consideration of a coarse change in time resolution about demand and PV generation. PV forecasting models suitable for the long-term, such as artificial intelligence, are usually less accurate when the time resolution is less than a few minutes [32]. Hence, the resolution for the coarse-grained loop can be rough, e.g., 15 minutes. Next, real-time control is performed to achieve a short-term energy balance in the fine-grained time scale between highly fluctuating renewable generation and fast-varying battery storage under the demand conditions derived from the longer-term planning loop. The time resolution in the fine-grained loop should be under few seconds for real-time control, managing the short-term variation of PV generation. This is because thermal time constants of PV cells are a few seconds and above [33], and the most critical battery's internal time constants are also above a few seconds. Clearly, the different problems an EMS framework deals with, appliance scheduling and demand load on the one hand and fluctuation of PV generation and battery operation, on the other hand, act on different time scales. However, the proposed framework still allows to treat of these problems in one integrated optimization loop, so not independently, as needed to obtain high accuracy in optimizing the balance.

Based on the above description, we formulate the multi-time scale structure for the smart PV system, as shown in Figure 2. Let t be a set of global time steps for the whole process, and the multi-time scale optimization is dispatched at every control point with a resolution Δt. Since the optimization problems are discretized in time, time windows (planning period) are divided by a given resolution. Firstly, a coarse-grained time scale with time index t_L, which corresponds to slower system dynamics, is designed to consider a daily variation of demand and PV generation. Thus, the coarse-grained time scale consists of the time window with a long planning period T_L with a resolution Δt_L; the typical value of them is: T_L is 24 hours, and Δt_L is 15 minutes. By solving a coarse-grained optimization, rough schedules of a smart PV system are obtained. Following the MPC approach, the solution of the only first Δt_L is usually applied to the system. In addition, the solution of the first Δt_L is interpolated in the finer grain to consider fast system behavior, such as real-time energy balancing. Therefore, after executing the coarse-grained optimization, the fine-grained time scale with time index t_S is performed. Keeping the time scale consistent, the planning period of fine-grained time scale T_S generally equals Δt_L. The time window is divided by fine resolution Δt_S, of which value is typically 1 second. Finally, as marked with the red window in Figure 2, the obtained solution is applied to the system.

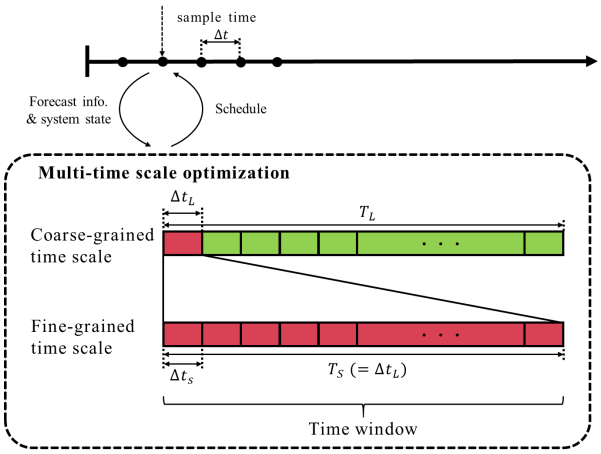

Figure 2: Schematic view of multi-time scale structure

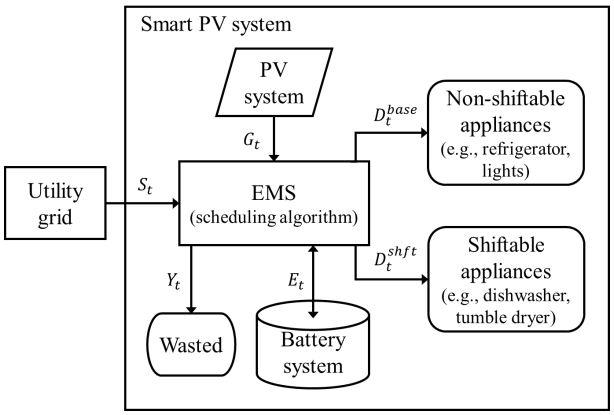

Figure 3: Smart PV system structure

3. Model Development

This section provides a detailed overview of the smart PV system and the mathematical model introduced in the proposed framework. Especially, a smart PV system model, a PV forecasting model, a battery model, and a smart appliance model are included. Hence, these main components will also be discussed in more detail.

3.1. Targeted smart PV system structure

The smart PV system is a local energy community which comprises several building and households. Figure 3 shows a schematic view of the smart PV system model. The main components of the smart PV system are PV panels and battery systems, especially the lithium-ion battery. The battery system is not only used to store the generated energy but also to supply the demand when (1) the energy generated by PV is not sufficient and (2) the EMS decides to supply the loads from the battery rather than the grid. It is assumed that there are two sets of appliances: non-shiftable appliances and shiftable appliances. The non-shiftable appliances are represented by a light, a refrigerator, etc., of which the starting time and its operation cannot be deferred and interrupted. On the other hand, the shiftable appliances are represented by a dishwasher, a washing machine, etc., of which the starting time can be shifted to the other time slot and would not be interrupted.

In the framework, both the battery system and shiftable appliances are scheduled to balance demand and PV production by solving an optimization problem with a constraint of user preferences. The EMS collects information on energy balance and system state from the smart PV system while managing overall energy flow based on the solution obtained by the framework shown in the previous section. The smart PV system buys the electricity from the utility grid in case of a power shortage. To prevent the grid instability by the reverse power flow, we assume that this system does not support selling the surplus generated energy to the utility grid. The surplus energy is consumed by smart appliances and battery as possible; otherwise, it is wasted inside the system.

In general, the energy balance inside the system must be kept at any time t, which is formulated by:

$$S_t + G_t + E_t = D_t^{base} + D_t^{shft} + Y_t, \quad \forall t \tag{1}$$

where S_t, G_t, and E_t denote the purchased energy from the utility grid, the generated energy of the PV system, and the charging/discharging energy of the battery, respectively. Let D_t^{base}, D_t^{shft}, and Y_t be the demand load of the non-shiftable appliances, the demand load of the smart appliances, and the wasted energy, respectively. The charging/discharging energy E_t takes a positive value when charging, and takes a negative value when discharging.

In addition, the purchased energy S_t and the wasted energy Y_t cannot be negative value as given by Eq.2 and Eq.3, respectively.

$$0 \leq S_{t_L}, \quad \forall t, \tag{2}$$

$$0 \leq Y_{t_L}, \quad \forall t. \tag{3}$$

It should be mentioned that this model does not consider other components such as wind turbine, the air conditioning system, and electric vehicle management, because this paper mainly focuses on the effect of PV forecasting and accurate battery model on the EMS performance. We can potentially add or remove other components by formulating their behavior mathematically. However, that is an ongoing work, and it would make this paper core way too complex to add all of these options in one disclosure.

3.2. Accurate physics-based PV forecasting model

The PV generation has a high fluctuation due to meteorological stochastic phenomena. Therefore, the real-time forecast data of PV generation is necessary to smooth the fluctuation by balancing demand and PV generation with battery scheduling. In this paper, we use the forecast data provided by the PV nowcasting model in [34], which can predict short-term generation based on sky-images, neural network model, and highly accurate physics-based modeling framework of Pv generators [35]. The major benefit of this model is that it is capable of providing PV energy forecasting with high temporal resolution. Also, the forecast is provided over a horizon of 15 minutes with a resolution of 1 second. Furthermore, the forecast can be updated

every minute. This is sufficient for iterating a fine-grained battery scheduling loop.

On the other hand, PV forecasting for the coarse-grained time scale is also important to take energy balance for long-term up to a few days. We assume that the PV forecasting data for a coarse-grained time scale is available online by a close-by meteorological station.

3.3. Appliance model

Each shiftable appliance is characterized by four parameters[36]: (1) operating time, (2) configuration time denoted by T^{conf}, which is the time to be able to start the appliance, (3) deadline denoted by T^{dead}, which is the time by which the appliance must be completed, and (4) electrical energy required by appliance operation. The shiftable appliance must be scheduled from the configuration time until the deadline. The scheduling problem is solved under user preferences, and the shiftable appliances automatically start based on the obtained solution.

A brief introduction of the formulation of the shiftable appliances is presented here. We model its operating cycle for each appliance. Let m be the index of the shiftable appliances. The operating time of each appliance is divided by the time resolution of Δt, and then, the index of each divided operating phase is represented by p. Where binary variables $q_{m,p,t}$ represent a state of the shiftable appliances; $q_{m,p,t} = 1$ if appliance m is in operation phase p at time t, otherwise 0. We also introduce binary variables $r_{m,p,t}$, which is a finish flag; $r_{m,p,t} = 1$ if operation phase p of appliance m is already finished at time t, otherwise 0. Besides, we can formulate the shiftable appliance scheduling as follows:

$$D_t^{shft} = \sum_{m=1}^{M} \sum_{p=1}^{P} q_{m,p,t} \cdot D_{m,p}^{app}, \quad \forall t, \tag{4}$$

$$q_{m,p,t} + r_{m,p,t} \leq 1, \quad \forall \{m, p, t\}, \tag{5}$$

$$q_{m,p,t-1} - q_{m,p,t} \leq r_{m,p,t}, \quad \forall \{m, p\},\ 2 \leq t \leq T, \tag{6}$$

$$r_{m,p,t-1} \leq r_{m,p,t}, \quad \forall \{m, p\},\ 2 \leq t \leq T, \tag{7}$$

$$q_{m,p,t} \leq r_{m,p-1,t}, \quad \forall \{m, t\},\ 2 \leq p \leq P, \tag{8}$$

$$r_{m,p-1,t} - r_{m,p,t} = q_{m,p,t}, \quad \forall \{m, t\},\ 2 \leq p \leq P, \tag{9}$$

$$\sum_{t=1}^{T} q_{m,p,t} = 1, \quad \forall \{m, p\}, \tag{10}$$

$$q_{m,p,t} = 0, \quad \forall \{m, p\},\ 1 \leq t \leq T_m^{conf},\ T_m^{dead} \leq t \leq T, \tag{11}$$

where $D_{m,p}^{app}$ is the demand energy of the phase p of appliance m. Eq.4 aggregates the shiftable demand. Eq.5-10 show the scheduling logic of the shiftable appliances. Eq.11 means the user preference about the timing of the appliance usage. This scheduling problem is solved at the coarse-grained time scale.

3.4. Accurate parameterized Battery model

Battery system models are very important tools for designing energy management systems in terms of scheduling and simulation. We would like to emphasize that the main contribution of this paper is to build a battery module model from battery cell model in [37] and leverage it to follow SOC profiles and charge-discharge loss accurately. As described in Section 1, most related studies have utilized a simple battery model that represents charging and discharging losses as linear and does not accurately capture the battery characteristics.

Assuming that each cell is identical in the battery module, the configuration of the battery module is shown in Figure 4. Here, N_s and N_p are a number of series-connected cells and a number of parallel-connected cells, respectively. We use the equivalent circuit model as a battery model that shows a good agreement with measurements of battery run-time and nonlinear I-V characteristics [37].

Based on [37], an aggregated equivalent circuit model of the battery module used in this paper is shown in Figure 5. The left part of the equivalent circuit expresses the battery lifetime. Here, a voltage source V_{SOC} represents the stored energy level of the battery, i.e., SOC, ranging from 0.0 (0%) to 1.0 (100%). A Terminal current of battery I_{batt} is positive when discharging and is negative when charging. In addition, the nominal capacity of the battery module, denoted by C_{nom}, is calculated from cell capacity C_{cell}:

$$C_{nom} = N_p \cdot C_{cell}, \tag{12}$$

and then, the change in SOC level is calculated based on the terminal current as follows:

$$SOC_{t+1} = SOC_t - \int_t^{t+1} \frac{I_{batt}}{C_{nom}} dt. \tag{13}$$

The right part of the equivalent circuit represents the I-V characteristics of the battery. The left parallel RC branch and the right one are in charge of shorter transient response and longer transient response of I-V characteristics, respectively. Here, a voltage source V_{batt} is the terminal voltage of the battery module. Each cell consists of an open circuit voltage V_{OC}, resistances (R_S, R_{TS}, R_{TL}), and capacitances (C_{TS}, C_{TL}). These parameters are a function of SOC level and given by:

$$\begin{aligned} V_{OC} &= a_1 \cdot \exp(a_2 \cdot SOC) + a_3 \\ &\quad + a_4 \cdot SOC + a_5 \cdot SOC^2 + a_6 \cdot SOC^3, \end{aligned} \tag{14}$$

$$R_S = a_7 \cdot \exp(a_8 \cdot SOC) + a_9, \tag{15}$$

$$R_{TS} = a_{10} \cdot \exp(a_{11} \cdot SOC) + a_{12}, \tag{16}$$

$$R_{TL} = a_{16} \cdot \exp(a_{17} \cdot SOC) + a_{18}, \tag{17}$$

$$C_{TS} = a_{13} \cdot \exp(a_{14} \cdot SOC) + a_{15}, \tag{18}$$

$$C_{TL} = a_{19} \cdot \exp(a_{20} \cdot SOC) + a_{21}, \tag{19}$$

where $\{a_n, \forall n = 1...21\}$ are the coefficients of the battery cell, and we use the values provided in the literature [37]. Finally, the terminal voltage V_{batt} and charge-discharge energy E in kWh are calculated by:

$$V_{batt} = N_s \cdot V_{OC} - I_{batt} \cdot \frac{N_s \cdot R_S}{N_p} - U_{TS} - U_{TL}, \tag{20}$$

$$E = I_{batt} \cdot V_{batt} / 1000 \tag{21}$$

where U_{TS} and U_{TL} are the voltage of the left parallel RC branch and the voltage of the right one, respectively, and they

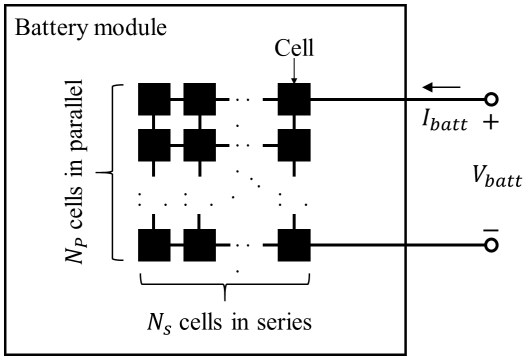

Figure 4: Configuration of battery module composed of N_s cells in series and N_p cells in parallel

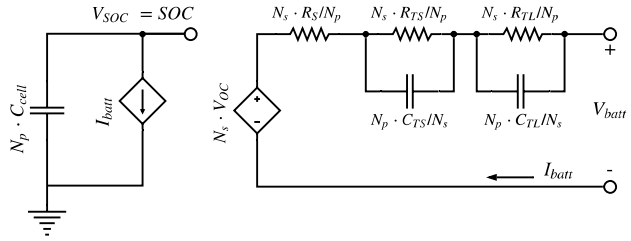

Figure 5: Equivalent circuit model of battery module

are calculated by following equations.

$$\frac{dU_{TS}}{dt} = -\frac{U_{TS}}{R_{TS} \cdot C_{TS}} + I_{batt} \cdot \frac{N_s}{N_p \cdot C_{TS}}, \tag{22}$$

$$\frac{dU_{TL}}{dt} = -\frac{U_{TL}}{R_{TL} \cdot C_{TL}} + I_{batt} \cdot \frac{N_s}{N_p \cdot C_{TL}}. \tag{23}$$

In this paper, the full equivalent circuit model is used in system simulation to estimate accurate battery states. Besides, the modified equivalent circuit model is implemented in the optimization problem to obtain effective battery utilization with reasonable computation time. The details of the modification of the battery model are described in the following section.

4. Mathematical Formulation of Multi-time Scale Optimization

The proposed framework's objective is to calculate optimal schedules of the smart PV system, which includes power purchase, the battery system, and the shiftable appliances. As mentioned in Section 2.2, the proposed framework employs a multi-time scale MPC composed of multiple optimization problems. Firstly, the optimization flow implemented in the proposed framework is shown, and then, we introduce a detailed mathematical formulation.

Figure 6 shows the multi-time scale optimization flow of the proposed framework. The optimization loop is composed of multiple optimization problems and executed in every internal period of Δt. First, coarse-grained time scale optimization is performed, and this time scale has two optimization problems: (1) the appliance scheduling (AS) and (2) the coarse-grained

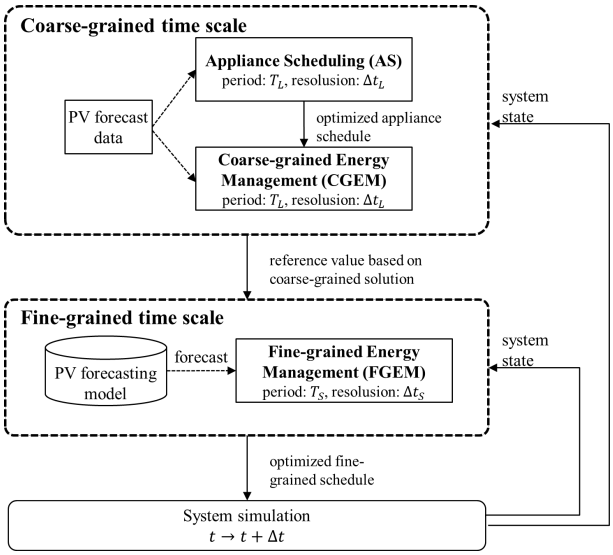

Figure 6: Multi-time scale optimization flow of proposed framework

energy management (CGEM). The AS problem is solved to decide the schedule of shiftable appliances. Besides, the CGEM problem is performed together with the obtained appliance schedule to calculate the reference solution of the battery. The CGEM includes the equivalent circuit battery model, and the battery characteristics are precisely considered. The planning period is still long at these optimizations, and the PV generation forecasting is roughly updated with coarse-grain resolution. After that, fine-grained time scale optimization is performed to decide precise control. PV forecasting model, mentioned in Sec3.2, generates the PV energy profiles, and fine-grained energy management (FGEM) optimization is solved together with forecast information and reference value obtained by the coarse-grained optimization. The reference value consists of the demand profiles of the shiftable appliances and battery energy profiles of charging and discharging. The fine-grain schedules of the battery system calculated by the FGEM are directly applied to the system. Based on optimal schedules, actual behavior is simulated with the full equivalent circuit battery model, and the battery state is updated. The formulation of the AS, CGEM, and FGEM is described in the following section.

4.1. Appliance scheduling

This section shows the detailed mathematical formulation of the AS. Because of the coarse-grained time scale, the time index is t_L with the time resolution of Δt_L. The problem includes some binary variables, and the AS is mixed-integer linear programming (MIP) problem; and the following formulation de-

scribes the optimization problem of AS:

$$\begin{aligned}
&\text{minimize} && \sum_{t_L=1}^{T_L} \xi_{t_L} \cdot S_{t_L}, && (24)\\
&\text{subject to} && (1)-(13),(21),\ \forall t_L,\\
&\text{input}\\
&&& \{G_{t_L}, D^{base}_{t_L}, \xi_{t_L}\},\ \forall t_L,\\
&\text{decision variables}\\
&&& \{S_{t_L}, Y_{t_L}, I_{batt,t_L}, q_{m,p,t_L}, r_{m,p,t_L}\},\ \forall\{m,p,t_L\},
\end{aligned}$$

where ξ_{t_L} is the electricity price of the power company in JPY (Japanese Yen) / kWh. Note that the AS employs the simplified battery model obtained by fixing the battery terminal voltage V_{batt} to the constant nominal value, i.e., the I-V characteristic of the battery is not considered in the AS. This is because the AS formulation includes integer variables, and the AS with the non-linear equivalent circuit is too complex to solve. This simplification is compensated in the following CGEM by re-solving the battery scheduling with the equivalent circuit model.

The objective is to minimize the electric bill, and the solution of the AS contains the optimal scheduling for the shiftable appliances, the battery, the wasted energy, and the power purchase from the utility grid. Only the optimal schedule of shiftable appliances, $D^{shft}_{t_L}$ and q_{m,p,t_L}, is applied to the system and other optimization; the rest are discarded and recalculated in the following problem.

4.2. Coarse-grained energy management

This section shows the detailed mathematical formulation of the CGEM. The CGEM is the outer loop for the battery scheduling considering the same time scale as AS.In the CGEM, the capacitances C_{TS} and C_{TL} are removed from the circuit model as shown in Figure5 because the dynamics of the transient response represented by these capacitances are very fast (20 seconds - 4 minutes). It does not make sense to consider these dynamics in the coarse-grained time scale. Hence, the battery equation is reformulated using resistance value R_{total}:

$$R_{total} = R_S + R_{TS} + R_{TL}, \tag{25}$$

$$V_{batt} = N_s \cdot V_{OC} - I_{batt} \cdot \frac{N_s \cdot R_{total}}{N_p}. \tag{26}$$

Because the CGEM includes non-linear equations of the battery model, the CGEM is a non-linear programming (NLP) problem. The formulation of the CGEM is finally described as follows:

$$\begin{aligned}
&\text{minimize} && \sum_{t_L=1}^{T_L} \xi_{t_L} \cdot S_{t_L}, && (27)\\
&\text{subject to} && (1)-(3),(12)-(17),(21),(25),(26),\ \forall t_L\\
&\text{input}\\
&&& \{G_{t_L}, D^{base}_{t_L}, D^{shft}_{t_L}, \xi_{t_L}\},\ \forall t_L,\\
&\text{decision variables}\\
&&& \{S_{t_L}, Y_{t_L}, I_{batt,t_L}\},\ \ \forall t_L,
\end{aligned}$$

where the objective is the same as the AS to minimize the electric bill. The solution of the CGEM contains the optimal scheduling for the battery, the wasted energy, and the power purchase from the utility grid.

The obtained battery schedule is more effective than the solution from the AS because the CGEM contains the equations that express the accurate I-V characteristics. The reference value of battery energy E^{ref} is input to the FGEM, as defined by:

$$E^{ref} = \frac{1}{1000} \cdot I^{batt}_1 \cdot V^{batt}_1 \cdot \frac{\Delta t_S}{3600}, \tag{28}$$

where the FGEM decides the fine-grained battery schedule based on E^{ref}, and this prevents the greedy solution of discharging anyway to minimize electric bill.

4.3. Fine-grained energy management

The FGEM is the inner loop for the battery scheduling to interpolate highly fluctuation of PV generation. The time index is t_S with the resolution of Δt_S, and the length of T_S normally equals the resolution Δt_L. In order to express the battery dynamics, i.e., the transient response, the full equivalent circuit of the battery module is employed. In addition, the battery trajectory in the fine-grained time scale should follow the schedules of the coarse-grained time scale. Thus, based on the reference value from the CGEM E^{ref}, the charging/discharging energy of the battery is constrained as formulated by Eq. (29).

$$E_{t_S} - E^{ref} \le \varepsilon \cdot |E^{ref}|, \forall t_S, \tag{29}$$

where ε denotes a relative error from the reference value, e.g., set to 5%.

Because the FGEM includes the non-linear equations of the battery model, the FGEM is an NLP problem. The following formulation finally shows the optimization problem of the FGEM:

$$\begin{aligned}
&\text{minimize} && \sum_{t_S=1}^{T_S} \xi_{t_S} \cdot S_{t_S}, && (30)\\
&\text{subject to} && (1)-(3),(12)-(14),(20)-(23),(29),\forall t_S,\\
&\text{input}\\
&&& \{G_{t_S}, D^{base}_{t_S}, D^{shft}_{t_S}, \xi_{t_S}\},\ \forall t_S,\\
&\text{decision variables}\\
&&& \{S_{t_S}, Y_{t_S}, I_{batt,t_S}\},\ \ \forall t_S,
\end{aligned}$$

where the AS solution for appliances D^{shft} is also input, and the objective is the same as the other problems to minimize the electric bill. The solution of the FGEM contains the optimal scheduling for the battery, the wasted energy, and the power purchase from the utility grid.

These optimal solutions are applied to the smart PV system, and the actual battery behavior is simulated with a complete equivalent circuit model in the system simulation. Note that the system simulation of the battery system is still a very important step in the real implementation. This is because the battery's internal state usually cannot be directly measured, and the simulation is required to estimate the battery state such as SOC accurately.

5. Simulation Results

In this section, we show several key simulation experiments to demonstrate the effectiveness of the proposed framework with practical assumptions. The experimental setup is firstly described, and then the case studies are performed under different settings of the proposed framework. Besides, the impact of PV forecasting error on the performance is also investigated. Finally, the proposed framework is compared with other baseline methods in terms of the electric bill.

5.1. Simulation setup

Firstly, the parameters of the proposed framework are shown here. In all experiments, the simulation period is ten days, and every simulation day starts at 0 a.m. The time resolution in the coarse- and fine-grained time scale are set to 15 minutes and 1 sec, respectively, i.e., $\Delta t_L = 900$ [sec] and $\Delta t_S = 1$ [sec]. The planning period of the coarse- and fine-grained time scale are set to 24hours and 15 minutes, respectively; thus, $T_L = 96$ [900sec] and $T_S = 900$ [sec]. The AS is a MIP problem and is solved by the commercial solver CPLEX [38]. The CGEM and FGEM are an NLP problem and is solved by the open-source solver IPOPT [39]. The computing platform utilized to run the simulation uses an Intel Core-i7 6600U CPU of 2 cores with a 2.60 GHz clock frequency and a 16 GB of DDR3 RAM.

The parameters of the battery in the optimization problems are described in Table 1. The electricity price is set to 21.66 JPY/kWh during daytime (7 a.m. - 11 p.m.) and 10.7 JPY/kWh during nighttime (11 p.m. - 7 a.m.). The peak power of the PV panel is set to 15 kWp. The PV generation profiles and other environmental data are collected at the University of Oldenburg over a period from June until July, 2015. Moreover, the fine-grained forecast of PV generation is provided by the PV forecasting model[34], of which the average forecasting error is less than 12%. The coarse-grained forecast of PV generation is manually generated by adding the error distribution to the real measured profiles, and its average error is 20%. On the other hand, the demand profiles of the non-shiftable appliances are based on the Dutch Residential Energy Dataset (DRED) [40], which are collected from July to December 2015. Here, the mean value of the demand load of the non-shiftable appliances per day is set to 12.5 kW. The shiftable appliances profiles are shown in Table 2. We use measured profiles given by the dataset[41]. It is assumed that there are four units of each smart appliance, which includes a washing machine, a tumble dryer, and a dishwasher, while each appliance is operated once a day. The configuration time is randomly generated within the range shown in Table 2, and the deadline is decided by adding the shiftable time to the configuration time. The actual electric bill is calculated by the system simulation to evaluate the proposed framework.

5.2. Comparison study with baseline methods

In this section, the proposed framework is compared with several representative baseline methods to evaluate the effectiveness of appliance and battery scheduling. The proposed framework is denoted by **Proposed**, and the baseline methods are described as follows:

1) **Using Shiftable Appliances As Soon As Possible (ASAP):** smart appliances are not scheduled by optimization. They are turned on as soon as the configuration time comes. The battery schedule is optimized by the CGEM and the FGEM.
2) **No Battery Scheduling (NBS):** the CGEM and FGEM are removed from the proposed method while the AS is solved. The battery is assumed to be charged with constant C-rate 10% during the nighttime (11 p.m. - 7 a.m.) and be discharged with constant C-rate 5% during the daytime (7 a.m. - 11 p.m.).
3) **ASAP-NBS:** this is a method that combines the ASAP and the NBS; thus, no optimization problem is solved.

Table 3 shows the results of the electric bill for 10 days and the improving rate of Proposed with respect to other methods. The result indicates that the proposed framework achieves the lowest electric bill in all methods, and the max improving rate of the electric bill is 48.1%. Appliance scheduling can fill the energy gap between generation and demand; thus, the electric bill is clearly reduced. Moreover, it is indicated that the major contributing factor in improving the electric bill is battery scheduling. When the battery is charged and discharged by constant current such as the NBS, the battery cannot control the balance between renewable generation and demand; as a result, the purchased energy increases in order to ensure the demand is fulfilled.

5.3. Impact of planning period for coarse-grained time scale

In this section, the impact of the planning period of the coarse-grained time scale is investigated. The proposed framework is performed with different planning periods T_L from 6 hours to 48 hours.

Table 1: Parameters of battery

Description	Symbol	Value
Initial SOC	SOC^{init}	0.5 (50%)
Terminal SOC	SOC^{term}	0.5 (50%)
Min. SOC	$\underline{SOC}$	0.2 (20%)
Max. SOC	$\overline{SOC}$	1 (100%)
Min. current	$\underline{I_{batt}}$	$-0.5 \cdot C_{nom}$ (50% of capacity)
Max. current	$\overline{I_{batt}}$	$0.5 \cdot C_{nom}$ (50% of capacity)
Nb. cells in series	N_s	25
Nb. cells in parallel	N_p	191
Nominal voltage	V_{cell}	4.1 [V]
Nominal capacity	C_{cell}	0.85 [Ah]
Battery capacity	-	15 [kWh]

Table 2: Profiles of smart appliances

Appliance	Total energy	Operation time	Conf. time	Shiftable time
Washing machine	0.22kWh	45min	8 a.m. - 10 a.m.	7hours
Tumble dryer	1.86kWh	75min	8 a.m. - 10 a.m.	7hours
Dishwasher	1.88kWh	75min	12 p.m. - 15 p.m.	8hours

Table 3: Results of electric bill for 10 days and improving rate of electric bill of proposed method compared to different methods

Method	Proposed	ASAP	NBS	ASAP-NBS
Electric bill for 10 days [JPY]	3004	3319	4408	5784
Improving rate of eletric bill of Proposed	-	9.5%	31.9%	48.1%

Table 4: Results of electric bill and computational time with different planning period

Planning period	Electric	Computational time {[}sec{]}}		
T_L	bill [JPY]	AS	CGEM	FGEM
6hours	3194	0.95	0.19	3.11
12hours	3106	1.63	0.27	3.03
24hours	3004	4.32	0.43	3.51
36hours	3044	8.65	0.63	3.12
48hours	3055	17.59	0.94	3.24

Table 4 shows the electric bill over ten days and the mean value of the computational time for each optimization problem. The electric bill is decreasing until the planning period increases to 24 hours. However, when the planning period is longer than 24 hours, the electric bill increases. On the other hand, the computational time of each optimization problem increases as the planning period increases. Especially when the planning period reaches 48 hours, the computational time of the AS significantly increases. This is because the longer the planning period, the higher the number of decision variables and smart appliances to be scheduled. However, since the sum of the computational time is much less than the length of time resolution Δt_L, the proposed framework is applicable for all the simulated planning periods. In addition, a daily (24hours) planning suits well with home and building applications because of the partly repetitive daily demands for the occupants. Therefore, when the planning period of the coarse-grained time scale should be set to 24 hours, the proposed framework achieves good performance.

5.4. Impact of number of smart appliances

The impact of the number of smart appliances on the computational time is demonstrated. All types of smart appliances are increased from 2 to 10, i.e., the total number of smart appliances is changed from 6 to 30. Each appliance is scheduled once a day; thus, the AS calculates the optimal schedule for 6 - 30 appliances per day.

Table 5 shows the average computational time for each optimization problem. Naturally, the computational time of the AS increases with the increase in the number of appliances. However, the requirement for the computational time, that every optimization flow must complete less than $\Delta t_L = 900$ sec, is always met, and the computational time is short enough. Thus, if the smart PV system has several buildings and many smart appliances such as 30 or more, the AS is sufficient in both accuracy and time complexity for the planning of the shiftable appliances.

Table 5: Results of average computation time under scenarios with different number of smart appliances

# shiftable appliances per day	Computational time [sec] AS
6	2.13
12	4.32
18	6.67
24	8.79
30	10.39

5.5. Impact of PV forecasting error and battery size

In this section, the proposed framework with different PV forecasting errors is performed in order to analyze the impact of the PV forecasting error on the electric bill. The average forecasting error of the PV forecasting in the coarse-grained time scale is set to 20, 30, or 40%. Moreover, in the fine-grained time scale, two different forecasting schemes are compared; energy forecasting proposed in [34] and power forecasting presented in [34] as a baseline method. The average forecasting errors for 15 minutes horizons of the energy and power forecasting are about 12% and 20%, respectively. As an ideal case, we employ the perfect forecasting method assumed that the forecasting error for both time scale is 0%. Besides, in order to investigate the effect of battery sizing, the battery capacity is also changed from 3kWh to 18kWh.

Figure 7 shows the results of the electric bill for various PV forecasting errors and battery capacities, and the detailed values of the electric bill are also shown in Table 6. In Figure 7, the black line indicates the electric bill in case of the perfect forecasting, and the red and blue line denotes that in case of the energy and power forecasting for fine-grained time scale, respectively. As can be seen from these results, the battery size is too large such as 18 kWh, the improvement of the electric bill is often saturated. On the other hand, looking at the forecasting error for the coarse-grained time scale, when the battery capacity is larger than 9kWh, the smaller the forecasting error, the lower the electric bill. However, when the battery capacity is 3 or 6 kWh, the prediction error of coarse-grain does not have much effect on the electricity bill. On the other hand, focusing on the PV forecasting scheme for the fine-grained time scale, the better forecasting scheme, i.e., the energy forecasting, greatly improves the electric bill. Therefore, it is clearly indicated that the accuracy of the forecasting scheme for the fine-grained time scale is a significant factor for the performance of the energy management. As a remarkable result, a 10% improvement in fine-grain forecast error is equivalent to a 30-50% reduction in battery size to achieve the same electric bill.

6. Summary

In this paper, an online multi-time scale energy management framework for a smart PV system is proposed. In the proposed framework, a model predictive control (MPC) approach is employed that uses PV generation forecasting as input to deal with the highly fluctuating PV generation. Moreover, the proposed framework solves three interconnected optimization problems

Table 6: Detailed values of electric bill for 10 days in JPY with different PV forecasting errors and battery capacities

Battery capacity	Perfect forecasting	Forecasting scheme for coarse-grained					
		Energy forecasting (error <12%)			Power forecasting (error <20%)		
		Forecast error for fine-grained			Forecast error for fine-grained		
		20%	30%	40%	20%	30%	40%
3kWh	3450	3558	3529	3579	3610	3570	3612
6kWh	3146	3309	3292	3360	3437	3404	3477
9kWh	3025	3181	3227	3272	3334	3381	3420
12kWh	2821	3037	3118	3171	3202	3289	3353
15kWh	2739	3004	3094	3185	3182	3271	3379
18kWh	2719	3027	3092	3205	3193	3281	3384

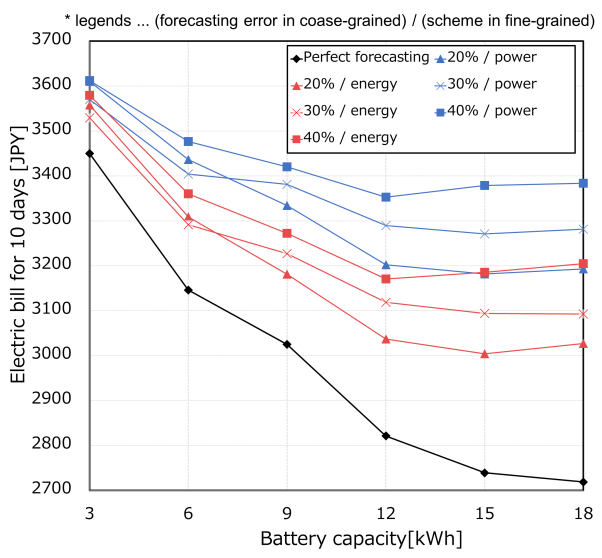

Figure 7: Results of electric bill for 10 days under scenarios with different PV forecasting errors and battery capacities

using the multi-time scale structure, considering long and short-term system dynamics simultaneously. The multi-time scale consists of two-time scales that are the coarse-grained and fine-grained time scale. In the coarse-grained time scale, the smart appliances are scheduled to shift the operating time; also, the battery charge/discharge profiles are optimized to deal with the daily variation of the PV generation and demand. In the fine-grained time scale, the battery's precise control is realized by introducing an accurate battery model that is combined with the fine-grained PV forecasting model. The results are compared with representative baseline methods and demonstrate that the proposed framework allows a reduction of the electric bill under different scenarios up to a maximum of 48.1%. Moreover, the impact of the PV forecasting error and the battery capacity on the performance of the proposed framework are investigated. If an accurate PV forecasting model is introduced, a significant reduction of the electric bill can be obtained even with small batteries. Therefore, the combination of accurate PV forecasting and the proposed energy management framework would lead to a reduction of the installation cost since a smaller battery system could be used. Future work includes extending the proposed framework to multi-objective optimization for maximizing user comfort and minimizing system cost. In particular, the HVAC system must be considered [42, 43, 44].

Acknowledgments

Funding: This work was supported by the European Union's Horizon 2020 research and innovation programme under the Marie Skłodowska-Curie grant agreement [grant number 751159].

References

[1] G. Pepermans, J. Driesen, D. Haeseldonckx, R. Belmans, W. D'haeseleer, Distributed generation: definition, benefits and issues, Energy Policy 33 (6) (2005) 787–798.

[2] R. H. Lasseter, P. Paigi, Microgrid: a conceptual solution, in: 2004 IEEE 35th Annual Power Electronics Specialists Conference, Vol. 6, 2004, pp. 4285–4290.

[3] N. Hatziargyriou, H. Asano, R. Iravani, C. Marnay, Microgrids, IEEE Power and Energy Magazine 5 (4) (2007) 78–94.

[4] C. Chen, S. Duan, T. Cai, B. Liu, G. Hu, Smart energy management system for optimal microgrid economic operation, IET Renewable Power Generation 5 (3) (2011) 258–267.

[5] L. Olatomiwa, S. Mekhilef, M. S. Ismail, M. Moghavvemi, Energy management strategies in hybrid renewable energy systems: A review, Renewable Sustainable Energy Reviews 62 (2016) 821–835.

[6] D. Mariano-Hernández, L. Hernández-Callejo, A. Zorita-Lamadrid, O. Duque-Pérez, F. Santos García, A review of strategies for building energy management system: Model predictive control, demand side management, optimization, and fault detect & diagnosis, Journal of Building Engineering 33 (2021) 101692.

[7] A. Merabet, K. Tawfique Ahmed, H. Ibrahim, R. Beguenane, A. M. Y. M. Ghias, Energy management and control system for laboratory scale microgrid based Wind-PV-Battery, IEEE Transactions on Sustainable Energy 8 (1) (2017) 145–154.

[8] D. Azuatalam, K. Paridari, Y. Ma, M. Förstl, A. C. Chapman, G. Verbič, Energy management of small-scale PV-battery systems: A systematic review considering practical implementation, computational requirements, quality of input data and battery degradation, Renewable Sustainable Energy Reviews 112 (2019) 555–570.

[9] A. Szumanowski, Y. Chang, Battery management system based on battery nonlinear dynamics modeling, IEEE Trans. Veh. Technol. 57 (3) (2008) 1425–1432.

[10] M. Killian, M. Zauner, M. Kozek, Comprehensive smart home energy management system using mixed-integer quadratic-programming, Appl. Energy 222 (January) (2018) 662–672.

[11] B. Celik, R. Roche, D. Bouquain, A. Miraoui, Decentralized neighborhood energy management with coordinated smart home energy sharing, IEEE Transactions on Smart Grid 9 (6) (2017) 6387–6397.

[12] T. Cui, S. Chen, Y. Wang, Q. Zhu, S. Nazarian, M. Pedram, An optimal energy co-scheduling framework for smart buildings, Integration, the VLSI Journal 58 (May) (2017) 528–537.

[13] H. S. Ganesh, K. Seo, H. E. Fritz, T. F. Edgar, A. Novoselac, M. Baldea, Indoor air quality and energy management in buildings using combined moving horizon estimation and model predictive control, Journal of Building Engineering 33 (2021) 101552.

[14] Y. Zhang, N. Rahbari-Asr, J. Duan, M.-Y. Chow, Day-ahead smart grid cooperative distributed energy scheduling with renewable and storage in-

tegration, IEEE Transactions on Sustainable Energy 7 (4) (2016) 1739–1748.
[15] S. Dorahaki, R. Dashti, H. R. Shaker, Optimal energy management in the smart microgrid considering the electrical energy storage system and the demand-side energy efficiency program, Journal of Energy Storage 28 (2020) 101229.
[16] A. Akbari-Dibavar, S. Nojavan, B. Mohammadi-Ivatloo, K. Zare, Smart home energy management using hybrid robust-stochastic optimization, Comput. Ind. Eng. 143 (2020) 106425.
[17] H. R. O. Rocha, I. H. Honorato, R. Fiorotti, W. C. Celeste, L. J. Silvestre, J. A. L. Silva, An artificial intelligence based scheduling algorithm for demand-side energy management in smart homes, Appl. Energy 282 (2021) 116145.
[18] N. A. Mohammed, A. Al-Bazi, Management of renewable energy production and distribution planning using agent-based modelling, Renewable Energy 164 (2021) 509–520.
[19] S. Bhattacharjee, C. Nandi, Design of a voting based smart energy management system of the renewable energy based hybrid energy system for a small community, Energy 214 (2021) 118977.
[20] F. A. Qayyum, M. Naeem, A. S. Khwaja, A. Anpalagan, L. Guan, B. Venkatesh, Appliance scheduling optimization in smart home networks, IEEE Access 3 (2015).
[21] J. Silvente, L. G. Papageorgiou, An MILP formulation for the optimal management of microgrids with task interruptions, Applied Energy 206 (2017) 1131–1146.
[22] Q. Lu, Z. Zhang, S. Lü, Home energy management in smart households: Optimal appliance scheduling model with photovoltaic energy storage system, Energy Reports 6 (2020) 2450–2462.
[23] A. Abreu, R. Bourdais, H. Guéguen, Hierarchical model predictive control for building energy management of hybrid systems, IFAC-PapersOnLine 51 (16) (2018) 235–240.
[24] A. Lefort, R. Bourdais, G. Ansanay-Alex, H. Guéguen, Hierarchical control method applied to energy management of a residential house, Energy and Buildings 64 (2013) 53–61.
[25] X. Jin, J. Wu, Y. Mu, M. Wang, X. Xu, H. Jia, Hierarchical microgrid energy management in an office building, Applied Energy 208 (2017) 480–494.
[26] M. Elkazaz, M. Sumner, E. Naghiyev, S. Pholboon, R. Davies, D. Thomas, A hierarchical two-stage energy management for a home microgrid using model predictive and real-time controllers, Appl. Energy 269 (2020) 115118.
[27] L. Ferrarini, G. Mantovani, G. T. Costanzo, A distributed model predictive control approach for the integration of flexible loads, storage and renewables, IEEE International Symposium on Industrial Electronics (2014) 1700–1705.
[28] A.-L. Klingler, L. Teichtmann, Impacts of a forecast-based operation strategy for grid-connected PV storage systems on profitability and the energy system, Solar Energy 158 (2017) 861–868.
[29] C. E. Garcia, D. M. Prett, M. Morari, Model predictive control: theory and practice - a survey, Automatica 25 (3) (1989) 335–348.
[30] G. R. Ruiz, E. L. Segarra, C. F. Bandera, Model predictive control optimization via genetic algorithm using a detailed building energy model, Energies 12 (1) (2019).
[31] A. Parisio, E. Rikos, L. Glielmo, A model predictive control approach to microgrid operation optimization, IEEE Transactions on Control Systems Technology 22 (5) (2014) 1813–1827.
[32] M. Diagne, M. David, P. Lauret, J. Boland, N. Schmutz, Review of solar irradiance forecasting methods and a proposition for small-scale insular grids, Renewable Sustainable Energy Reviews 27 (2013) 65–76.
[33] H. Goverde, D. Anagnostos, B. Herteleer, J. Govaerts, K. Baert, B. Aldalali, F. Catthoor, J. Driesen, J. Poortmans, Model requirements for accurate short term energy yield predictions during fast-varying weather conditions, in: 31st European Photovoltaic Solar Energy Conference and Exhibition (EUPVSEC), 2015, pp. 1556–1559.
[34] D. Anagnostos, S. Thomas, S. Cavadias, D. Soudris, J. Poortmans, F. Catthoor, A method for detailed, short-term energy yield forecasting of photovoltaic installations, Renewable Energy 130 (2019) 122–129.
[35] H. Goverde, D. Anagnostos, J. Govaerts, P. Manganiello, E. Voroshazi, K. Baert, J. Szlufcikl, F. Catthoor, J. Poortmans, J. Driesen, Accurately simulating PV energy production: Exploring the impact of module Build-Up, in: 33rd European Photovoltaic Solar Energy Conference and Exhibition, 2017, pp. 1643–1646.
[36] N. Sadeghianpourhamami, T. Demeester, D. F. Benoit, M. Strobbe, C. Develder, Modeling and analysis of residential flexibility: timing of white good usage, Applied energy 179 (2016) 790–805.
[37] M. Chen, G. A. Rincón-Mora, Accurate electrical battery model capable of predicting runtime and I-V performance, IEEE Transactions on Energy Conversion 21 (2) (2006) 504–511.
[38] IBM ILOG CPLEX v12.10, https://www.ibm.com/products/ilog-cplex-optimization-studio, [Online; accessed 1-Nov-2020] (2020).
[39] A. Wächter, L. T. Biegler, On the implementation of an interior-point filter line-search algorithm for large-scale nonlinear programming, Mathematical Programming 106 (1) (2006) 25–57.
[40] S. N. Akshay Uttama Nambi, A. R. Lua, R. V. Prasad, LocED: location-aware energy disaggregation framework, in: the 2nd ACM International Conference on Embedded Systems For Energy-Efficient Built Environments (BuildSys), 2015, pp. 45–54.
[41] A. Reinhardt, P. Baumann, D. Burgstahler, M. Hollick, H. Chonov, M. Werner, R. Steinmetz, On the accuracy of appliance identification based on distributed load metering data, in: the 2012 Sustainable Internet and ICT for Sustainability (SustainIT), 2012, pp. 1–9.
[42] A. Afram, F. Janabi-Sharifi, Gray-box modeling and validation of residential HVAC system for control system design, Applied Energy 137 (2015) 134–150.
[43] P. O. Fanger, Thermal comfort: analysis and applications in environmental engineering, Danish Technical Press, 1970.
[44] H. Shi, Q. Chen, Building energy management decision-making in the real world: A comparative study of HVAC cooling strategies, Journal of Building Engineering 33 (2021) 101869.